

Li⁺ adsorption at prismatic graphite surfaces enhances interlayer cohesion

Lars Pastewka^{a,b,*}, Sami Malola^c, Michael Moseler^{a,d,e}, Pekka Koskinen^c

^a*Fraunhofer-Institut für Werkstoffmechanik IWM, Wöhlerstraße 11, 79108 Freiburg, Germany*

^b*Department of Physics and Astronomy, Johns Hopkins University, 3400 North Charles Street, Baltimore, MD 21218, USA*

^c*NanoScience Center, Department of Physics, 40014 University of Jyväskylä, Finland*

^d*Freiburger Materialforschungszentrum, Albert-Ludwigs Universität, Stefan-Meier-Straße 21, 79104 Freiburg, Germany*

^e*Physikalisches Institut, Albert-Ludwigs Universität, Hermann-Herder-Straße 3, 79104 Freiburg, Germany*

Abstract

We use density functional calculations to determine the binding sites and binding energies of Li⁺ at graphene edges and prismatic graphite surfaces. Binding is favorable at bare and carbonyl terminated surfaces, but not favorable at hydrogen terminated surfaces. These findings have implications for the exfoliation of graphitic anodes in lithium-ion batteries that happens if solute and solvent co-intercalate. First, specific adsorption facilitates desolvation of Li⁺. Second, chemisorption lowers the surface energy by about 1 J m⁻² prismatic surface area, and gives graphite additional stability against exfoliation. The results offer an explanation for experiments that consistently show exfoliation for hydrogenated graphite, but show no exfoliation for oxygenated graphite.

Keywords: graphite, lithium, surface chemistry, exfoliation, anode, density-functional calculation

*Corresponding author

Email address: lars.pastewka@iwm.fraunhofer.de (Lars Pastewka)

1. Introduction

Over the past three decades, lithium-ion batteries have been established for high density storage of electrical energy [1, 2]. A fresh battery is formed during the first charge-discharge cycle where the organic electrolyte [3] decomposes at the electrodes' surfaces and reacts to form an ambiguous phase of matter called the solid electrolyte interphase (SEI) [4]. It is believed that the SEI acts as a solid-state electrolyte and sieve that selectively allows conduction of the Li^+ cation, but not the solvent [4]. This then passivates the anode against further reactions with the electrolyte. For graphite, the most common anode material, this sieving function of the SEI is believed to also prevent co-intercalation of cation and solvent that is accompanied by exfoliation of the graphite [4, 5, 6, 7]. This idea is usually corroborated by the fact that SEI formation occurs at $\sim 0.8\text{-}1.0\text{ V vs. Li/Li}^+$ while exfoliation is observed at $\sim 0.4\text{ V vs. Li/Li}^+$ — hence after the SEI has formed [8]. Charge consumption during exfoliation is linked to the creation of a SEI at the newly created basal surfaces [7].

However, experiments show a correlation between surface chemistry and exfoliation that is difficult to understand from this picture: Oxygenation of graphite suppresses exfoliation, while electrodes heat-treated with hydrogen exfoliate within the first charge cycles [8, 9, 10]. Yet, a SEI forms on both oxygenated and hydrogenated prismatic surfaces as well as on basal planes. The different exfoliation behavior is then usually related to the difference in SEI structure that is found on these surfaces [4]. Mechanistic details of this protective function of the SEI are still elusive. Here, we propose a mechanism that relates the exfoliation of the compound to the graphite's surface chemistry and is independent of SEI structure.

We carried out density functional theory (DFT) calculations that show that specific adsorption of Li^+ at pristine and oxygenated prismatic graphite enhances the interlayer cohesion energy by about 1 J m^{-2} , while no such enhancement is found for hydrogenated graphite. We propose that this additional interplanar binding acts as a glue that protects the graphite against exfoliation. These results suggest that tailoring the surface chemistry of the anode could enhance the cyclability of common lithium-ion batteries.

Our suggestion originates in the observation that because surface functional groups have such a crucial influence on graphite exfoliation, the anode surface must play a role in addition to being a source of electrons for intercalation and electrolyte reduction reactions. Prismatic graphite surfaces are electrochemically active [11]. In water-based electrolytes, basal planes show only residual activity that can be linked to the presence of defects and step edges [12]. Similarly, DFT calculations show only weak Li^+ binding at basal surfaces of graphite [13, 14] and graphene [15, 16]. The intercalation reaction itself proceeds on prismatic surfaces, or possibly defects on basal surfaces. If the Li^+ loses its solvation shell during this reaction, then there must be an intermediate reaction step where the cation is chelated at the surface that is energetically favored over the solvated situation. Indeed, such chelated configurations have been observed in first-principles (DFT) molecular dynamics simulations on the initial stages of SEI formation [17]. We here follow this idea and compute the chemical potential of Li^+ at prismatic graphite surfaces using DFT.

2. Computational methods

We compute total energies using spin-polarized DFT with the Perdew-Burke-Ernzerhof (PBE) generalized gradient approximation for the exchange-correlation functional [18]. The core electrons are treated in the projector-augmented wave formalism [19]. Density and wave-functions are expanded on a real-space grid as implemented in the GPAW code [20]. In all cases, we use a grid spacing of less than 0.20 Å and more than 6.0 Å vacuum in the non-periodic directions. Formation and adsorption energies on edges are computed from graphene ribbons with a width of 18 Å for ac and 20 Å for zz edges where edge formation energies are well converged [21]. All configurations are symmetric and have a vanishing net dipole moment. We use 10 k-points in the periodic direction within the basal planes for a unit-cell with two surface carbons. For graphite, $4n^{-1}$ k-points are used perpendicular to the basal planes where n is the number of graphene layers. Because the PBE functional does not capture van-der-Waals interactions, the graphite interlayer spacing was fixed to the experimental value of 3.355 Å. Along the edge direction, the unit cell size was fixed to conform with an intralayer lattice constant of 4.26 Å. This value is the lattice constant of a graphene sheet at zero external stress obtained from the particular DFT methodology that is used throughout this paper. Ground state configurations were found by minimizing the total energy using the fast inertial relaxation engine [22] until forces are converged to below 0.05 eV/Å.

The relative stability of the individual adsorption scenarios can be quantified by the Gibbs free energy difference ΔG . The reference configuration is the bcc bulk lithium metal that is used as a reference in most experiments. Using bcc lithium as a reference has yielded ab-initio intercalation voltages for cathodes

to within 0.1 V of the experimental values [23]. For inorganic solid state systems where pressure, thermal and configurational entropy contributions can be neglected, the formation energy is typically a good approximation to the Gibbs free energy [24, 23]. We approximate $G_X^f = E_X^{\text{tot}}$ where E_X^{tot} is the total energy of compound X as obtained from our DFT calculations. The Gibbs free energy difference for the formation of the adsorbed configuration is given by

$$\Delta G_{X;\text{Li}}^f = n_{\text{Li}}\mu_{\text{Li};X} = E_{X;\text{Li}}^{\text{tot}} - E_X^{\text{tot}} - n_{\text{Li}}E_{\text{Li,bulk}}^{\text{tot}}, \quad (1)$$

where X denotes the adsorbate and n_X is the number of adsorbate atoms per unit cell. Specifically, E_X^{tot} is the total energy of the bare surface X , $E_{X;\text{Li}}^{\text{tot}}$ is the energy of the surface including the adsorbed lithium, and $E_{\text{Li,bulk}}^{\text{tot}}$ is the energy per atom in a reference bcc lithium crystal. With these definitions $\mu_{X;\text{Li}}$ is the lithium chemical potential. Note that we find the cohesive energy of bulk bcc lithium as 1.68 eV per atom in excellent agreement with experiments [25]. For lithium uptake into bulk graphite we obtain a chemical potential of -0.04 eV compared to -0.15 eV for LDA calculations [26] and room temperature experiments [27].

3. Results and discussion

In addition to the bare chemical potentials μ , we compute the change in interlayer cohesion due to Li^+ chemisorption that is a measure for the stability of the layered compound against exfoliation. The surface contribution to interlayer cohesion of the graphite crystal is:

$$\Delta\gamma = (\mu_{\text{Li,graphite}} - \mu_{\text{Li,graphene}})/A_{\text{Li}}. \quad (2)$$

Here, $\Delta\gamma$ is the gain in surface energy due to Li^+ adsorption, where A_{Li} is the surface area occupied by a single Li^+ on the prismatic plane. We note that errors

in the bulk interlayer van-der-Waals interaction cancel in Eq. (2). To evaluate the quantity $\Delta\gamma$ we need the chemical potential μ of Li^+ at graphene (fully exfoliated graphite) and graphite surfaces.

We start by computing the chemical potential of lithium relative to the bcc bulk metal at graphene armchair (ac) and zig-zag (zz) edges. Contrary to previous studies [15, 28] we look for configurations at the edge and not on top of the honeycomb lattice near the edge. The ground state geometries for adsorption at bare edges are summarized in Fig. 1. The chemical potential (black squares in Fig. 1) varies between -2.0 to 0 eV for all configurations that were studied and is highest for ac edges and lowest for zz edges. For a specific type of edge, lower chemical potentials are obtained at half coverage (one Li^+ for every second sp carbon). Zig-zag edges have the lowest edge density with one Li^+ per 2.46 \AA while ac edges have one Li^+ per 2.13 \AA . The Li^+ has a Bader charge [29] of about $0.9|e|$ in all situations studied in this paper. The energy due to electrostatic repulsion of adjacent Li^+ is hence lowest for zz edges. To quantify a covalent contribution to bonding, we also investigated reconstructed zig-zag (rz) edges that are self-passivated [21]. These have the same edge density as zz edges, but show lithium chemical potentials close to zero and hence higher than ac edges. The order of chemical potentials (rz showing weakest and zz strongest binding) is identical to the results obtained for hydrogen termination [21]. We conclude that the C-Li bond at zz and ac edges has a significant covalent contribution that is suppressed at rz edges. Yet, the cation attains a position that would correspond to a hollow site if the crystal was continued through the edge which is indicative of ionic binding. At half-coverage the ions sit in the plane of the graphene, but due to repulsion of neighboring lithiums they deviate out of plane at full coverage.

The chemical potentials shown in Fig. 1 are computed with respect to un-terminated graphite surfaces. Ideal edges with dangling bonds rarely exist in nature, but the configurations shown in the top insets of Fig. 1 could be the product of an electrophilic substitution reaction or a reactive intermediate. Most oxygenated edges are found to be terminated by organic functional groups such as carbonyl, phenolic OH, lactones, ethers and carboxylates [30, 31]. To quantify the influence of a select terminal group we probed the chemisorption of Li^+ at edges terminated with carbonyl [17]. The bottom of Fig. 1 shows the resulting configurations. In all cases, the Li^+ is chelated between two oxygens. As for bare edges, the lithium sits in the plane at half-coverage but is forced to deviate out of plane for full coverage. The chemical potentials (red spheres in Fig. 1) are in the range of -1.5 eV to -3.0 eV and consistently lower than that for bare edges. Again, we find that half-coverage is more stable than full coverage, but the dependence on the type of edge disappears. We also find that Li^+ chemisorption changes the character of the C-O bond. Without any Li^+ , we find a bond length of 1.25 Å that corresponds to a C=O double bond. At half-coverage, that bond length extends to 1.28 Å and at full coverage we find 1.35 Å. The latter bond length is characteristic for a C-O single bond. This shows that Li^+ binds covalently to the oxygen in a manner that is similar to the isoelectric hydrogen.

We also probed hydrogen-terminated graphene edges, but were unable to find stable edge binding sites for any of the situations studied. The Li^+ needs to move onto the plane of the graphene in order to find a stable chemisorption position. In particular we find a repulsive chemical potential of 0.50 eV for chemisorption on top of the outermost hexagon of an armchair edge, and -0.04 eV for chemisorption near a zig-zag edge. These values are in excellent agreement with the results

reported by Uthaisar et al. [15], but show that Li^+ barely favors adsorption near zig-zag edges over bulk metal formation.

The situation for prismatic graphite surfaces is similar to graphene edges. The cations form a 2D ionic layer that shares the symmetry of the underlying graphite lattice. For AA stacked graphite this symmetry is cubic, while for AB stacked graphite the symmetry is a distortion of a hexagonal lattice. Chemical potentials are consistently about 1 eV lower than for graphene (Fig. 2). The values here are consistent with a value of -2.4 eV reported by Leung & Budzien for the AA stacked zz surface in the presence of an electrolyte [17]. This agreement indicates that solvation effects on the Li^+ chemical potential are negligible. As for the graphene edges, the presence of the terminal groups removes the dependency of the chemical potential on the crystallographic orientation of the surface (Fig. 2). In the AA and AB case the Li^+ is chelated by four and three oxygens, respectively.

In all calculations of AB stacked surfaces, we fixed the positions of the bulk carbon atoms and let only the outermost layer of carbons relax. Without this constraint, the lattice deforms and relaxes towards an AA stacked configuration. This observation indicates that staging [6] during graphite intercalation might nucleate at the surfaces. It is consistent with the result that Li^+ binds more strongly to AA stacked edges, and hints that the barrier for conversion may be low.

Our data shows that chemisorption at graphite surfaces is an energetically highly favorable process. The chemical potentials are in the range of common cathode materials such as LiCoO_2 (-3.75 eV) or LiMnO_2 (-3.13 eV) [23]. These energies suggest that chemisorption could be accompanied by substitution reactions. The products of typical anodic reduction reactions, like lithium ethylene dicarbonate [32], have liquid components that remain in the vicinity of the elec-

trode and could easily participate in such reactions.

Finally, we are in a position to compute the surface contribution to cohesion, $\Delta\gamma$. Results for the prismatic surfaces studied here are shown in Fig. 3. All energies are negative because the chemical potential μ shown in Figs. 1 and 2 is consistently lower for the graphite edge than it is for the graphene edge. This means the crystal becomes more stable and is effectively glued together by the adsorbed Li^+ . The values obtained here are of the same order of magnitude as surface energies of metals [33], albeit with opposite sign.

The influence of this surface contribution to full interlayer cohesion of the crystal depends on the surface to volume ratio. The total interlayer cohesion energy is given by $E_{\text{interlayer}} = E_{\text{vdW}} + A_{\text{pr}}\Delta\gamma$ where E_{vdW} is the binding energy due to the interlayer van-der-Waals interaction and A_{pr} the total prismatic surface area. Experimental values on the bulk interlayer cohesion energy e_{vdW} are rare in the literature. The values reported range from 35 ± 10 meV/atom (study of collapsed nanotubes [34]) over 43 meV/atom (heat of wetting [35]) to 52 ± 5 meV/atom (thermal desorption of polyaromatic hydrocarbons [36]). Recent high-level quantum calculations [37] report a value of ≈ 50 meV/atom. AA stacked graphite is about 15 meV/atom less stable than AB stacked graphite [38]. We therefore use an approximate intermediate value of $e_{\text{vdW}} = -40$ meV/atom that reflects some disorder through a mixture of AB and AA stacking in our estimates. If we cut a piece of graphite into a cube with two faces exposing the basal plane, we get four faces with prismatic surfaces. We thus assume that two-thirds of the accessible surface area is prismatic. Using the mass $m_{\text{C}} \approx 12$ g mol $^{-1}$ of a carbon atom we find for the total cohesive energy

$$E_{\text{interlayer}} \approx \frac{M}{m_{\text{C}}} e_{\text{vdW}} + \frac{2}{3} A \Delta\gamma. \quad (3)$$

The first term is the bulk contribution and the second the contribution of a surface of area A to the interlayer cohesion of an anode particle of mass M . Since prismatic surfaces are usually “heterogeneous and rough” [4] the true configurations will be more disordered than the idealized cases shown in Fig. 2. We therefore use a representative value of $\Delta\gamma = -1 \text{ J m}^{-2}$ to estimate that surface and bulk contributions in Eq. (3) become equal at specific surface areas of $A/M \approx 500 \text{ m}^2 \text{ g}^{-1}$. Pristine graphite has a BET surface area of around $5\text{-}20 \text{ m}^2 \text{ g}^{-1}$ [39]. The surface term then increases the cohesive energy by about 1-4%. Porous graphitic carbons can reach values in excess of $200 \text{ m}^2 \text{ g}^{-1}$ [40, 41]. For these structures the cohesive energy can increase by up to 50%. This lends them excess stability and makes exfoliation unlikely.

4. Conclusions

We have shown that lithium binds to bare and oxygen terminated graphene edges and graphite surfaces with chemical potentials of up to -4 eV with respect to bulk bcc lithium. We do not find stable binding at hydrogen terminated surfaces. The chemical potentials for bare surfaces and oxygen termination are comparable to those found in common cathode materials. Chelation of Li^+ at such surface sites must be an intermediate step when the cations move from the solution into the bulk of the intercalation compound to form LiC_6 . Strong binding at the surface therefore facilitates desolvation of the ions. We have also shown that Li^+ at prismatic graphite surfaces stabilizes interlayer cohesion. This surface contribution doubles the interplanar cohesion energy of the graphite crystal at a specific surface area of about $500 \text{ m}^2 \text{ g}^{-1}$. Both mechanisms prevent co-intercalation of Li^+ and solvent. We here propose that they could be an explanation why graphite

exfoliates when hydrogen-terminated, but does not exfoliate when treated in an oxygen atmosphere [8, 9, 10]. Such a mechanism would suggest that exfoliation and SEI formation are two unrelated processes, and that a sieving function of the SEI may be irrelevant for the suppression of exfoliation.

Acknowledgements

We thank Tommi Järvi, Kai-Christian Möller and Henning Lorrmann for useful discussions. This work was supported by the German BMBF (grants 03SF0343G and 13N10597). P.K. acknowledges funding from the Academy of Finland (grant 251216). L.P. acknowledges funding from the European Commission (HPC-Europa2, grant 228398) and thanks the University of Jyväskylä for hospitality. Computations were carried out at CSC Espoo and the Jülich Supercomputing Center.

- [1] C. Daniel, J. O. Besenhard, Handbook of Battery Materials, Wiley-VCH, 2011.
- [2] N.-S. Choi, Z. Chen, S. a. Freunberger, X. Ji, Y.-K. Sun, K. Amine, G. Yushin, L. F. Nazar, J. Cho, P. G. Bruce, Angew. Chem. Int. Ed. 51 (2012) 9994–10024. doi:10.1002/anie.201201429.
- [3] K. Xu, Chem. Rev. 104 (2004) 4303–4418. doi:10.1021/cr030203g.
- [4] M. Winter, Z. Phys. Chem. 223 (2009) 1395–1406. doi:10.1524/zpch.2009.6086.
- [5] J. O. Besenhard, M. Winter, J. Yang, W. Biberacher, J. Power Sources 54 (1995) 228–231. doi:10.1016/0378-7753(94)02073-C.

- [6] M. Winter, J. O. Besenhard, M. E. Spahr, P. Novák, *Adv. Mater.* 10 (1998) 725–763. doi:10.1002/(SICI)1521-4095(199807)10:10<725::AID-ADMA725>3.0.CO;2-Z.
- [7] R. Fong, U. von Sacken, J. R. Dahn, *J. Electrochem. Soc.* 137 (1990) 2009–2013. doi:10.1149/1.2086855.
- [8] S. H. Ng, C. Vix-Guterl, P. Bernardo, N. Tran, J. Ufheil, H. Buqa, J. Dentzer, R. Gadiou, M. E. Spahr, D. Goers, *Carbon* 47 (2009) 705–712. doi:10.1016/j.carbon.2008.11.008.
- [9] M. E. Spahr, H. Wilhelm, T. Palladino, N. Dupont-Pavlovsky, D. Goers, F. Joho, P. Novák, *J. Power Sources* 119-121 (2003) 543–549. doi:10.1016/S0378-7753(03)00284-2.
- [10] M. E. Spahr, H. Wilhelm, F. Joho, J.-C. Panitz, J. Wambach, P. Novák, N. Dupont-Pavlovsky, *J. Electrochem. Soc.* 149 (2002) A960–A966. doi:10.1149/1.1486238.
- [11] T. Placke, V. Siozios, R. Schmitz, S. F. Lux, P. Bieker, C. Colle, H.-W. Meyer, S. Passerini, M. Winter, *J. Power Sources* 200 (2012) 83–91. doi:10.1016/j.jpowsour.2011.10.085.
- [12] T. J. Davies, M. E. Hyde, R. G. Compton, *Angew. Chem. Int. Ed.* 44 (2005) 5121–5126. doi:10.1002/ange.200462750.
- [13] K. Rytönen, J. Akola, M. Manninen, *Phys. Rev. B* 75 (2007) 075401. doi:10.1103/PhysRevB.75.075401.

- [14] F. Valencia, A. H. Romero, F. Ancilotto, P. L. Silvestrelli, *J. Phys. Chem. B* 110 (2006) 14832–14841. doi:10.1021/jp062126+.
- [15] C. Uthaisar, V. Barone, J. E. Peralta, *J. Appl. Phys.* 106 (2009) 113715. doi:10.1063/1.3265431.
- [16] M. Khantha, N. Cordero, L. Molina, J. A. Alonso, L. A. Girifalco, *Phys. Rev. B* 70 (2004) 125422. doi:10.1103/PhysRevB.70.125422.
- [17] K. Leung, J. L. Budzien, *Phys. Chem. Chem. Phys.* 12 (2010) 6583–6586. doi:10.1039/B925853A.
- [18] J. P. Perdew, K. Burke, M. Ernzerhof, *Phys. Rev. Lett.* 77 (1996) 3865–3868. doi:10.1103/PhysRevLett.77.3865.
- [19] P. E. Blöchl, *Phys. Rev. B* 50 (1994) 17953. doi:10.1103/PhysRevB.50.17953.
- [20] J. J. Mortensen, L. B. Hansen, K. W. Jacobsen, *Phys. Rev. B* 71 (2005) 35109. doi:10.1103/PhysRevB.71.035109, we use GPAW version 0.8.0 and the default PAW setups version 0.6.6300. See: <https://wiki.fysik.dtu.dk/gpaw/>.
- [21] P. Koskinen, S. Malola, H. Häkkinen, *Phys. Rev. Lett.* 101 (2008) 115502. doi:10.1103/PhysRevLett.101.115502.
- [22] E. Bitzek, P. Koskinen, F. Gähler, M. Moseler, P. Gumbsch, *Phys. Rev. Lett.* 97 (2006) 170201. doi:10.1103/PhysRevLett.97.170201.
- [23] M. K. Aydinol, A. F. Kohan, G. Ceder, K. Cho, J. Joannopoulos, *Phys. Rev. B* 56 (1997) 1354–1365. doi:10.1103/PhysRevB.56.1354.

- [24] C. G. van de Walle, J. Neugebauer, *J. Appl. Phys.* 95 (2004) 3851–3879. doi:10.1063/1.1682673.
- [25] T. B. Douglas, L. F. Epstein, J. L. Dever, W. H. Howland, *J. Am. Chem. Soc.* 77 (1955) 2144–2150. doi:10.1021/ja01613a031.
- [26] K. R. Kganyago, P. E. Ngoepe, C. R. A. Catlow, *Solid State Ionics* 159 (2003) 21–23. doi:10.1016/S0167-2738(02)00763-4.
- [27] V. V. Avdeev, A. P. Savchenkova, L. A. Monyakina, I. V. Nikol'skaya, A. V. Khvostov, *J. Phys. Chem. Solids* 57 (1996) 947–949. doi:10.1016/0022-3697(95)00380-0.
- [28] C. Uthaisar, V. Barone, *Nano Lett.* 10 (2010) 2838–2842. doi:10.1021/nl100865a.
- [29] G. Henkelman, A. Arnaldsson, H. Jónsson, *Comput. Mater. Sci.* 36 (2006) 354–360. doi:10.1016/j.commatsci.2005.04.010.
- [30] R. L. McCreery, *Chem. Rev.* 108 (2008) 2646–2687. doi:10.1021/cr068076m.
- [31] R. I. R. Blyth, H. Buqa, F. P. Netzer, M. G. Ramsey, J. O. Besenhard, P. Golob, M. Winter, *Appl. Surf. Sci.* 167 (2000) 99–106. doi:10.1016/S0169-4332(00)00525-0.
- [32] G. V. Zhuang, K. Xu, H. Yang, T. R. Jow, P. N. Ross Jr., *J. Phys. Chem. B* 109 (2005) 17567–17573. doi:10.1021/jp052474w.
- [33] L. Vitos, A. V. Ruban, H. L. Skriver, J. Kollár, *Surf. Sci.* 411 (1998) 186–202. doi:10.1016/S0039-6028(98)00363-X.

- [34] L. X. Benedict, N. G. Chopra, M. L. Cohen, A. Zettl, S. G. Louie, V. H. Crespi, *Chem. Phys. Lett.* 286 (1998) 490–496. doi:10.1016/S0009-2614(97)01466-8.
- [35] L. A. Girifalco, R. A. Lad, *J. Chem. Phys.* 25 (1956) 693–697. doi:10.1063/1.1743030.
- [36] R. Zacharia, H. Ulbricht, T. Hertel, *Phys. Rev. B* 69 (2004) 155406. doi:10.1103/PhysRevB.69.155406.
- [37] T. Björkman, A. Gulans, A. V. Krasheninnikov, R. M. Nieminen, *Phys. Rev. Lett.* 108 (2012) 235502. doi:10.1103/PhysRevLett.108.235502.
- [38] A. N. Kolmogorov, V. H. Crespi, *Phys. Rev. B* 71 (2005) 235415. doi:10.1103/PhysRevB.71.235414.
- [39] F. Joho, B. Rykart, A. Blome, P. Novák, H. Wilhelm, M. E. Spahr, *J. Power Sources* 97-98 (2001) 78–82. doi:10.1016/S0378-7753(01)00595-X.
- [40] Y.-S. Hu, P. Adelhelm, B. M. Smarsly, S. Hore, M. Antonietti, J. Maier, *Adv. Funct. Mater.* 17 (2007) 1873–1878. doi:10.1002/adfm.200601152.
- [41] K. T. Lee, J. C. Lytle, N. S. Ergang, S. M. Oh, A. Stein, *Adv. Funct. Mater.* 15 (2005) 547–556. doi:10.1002/adfm.200400186.

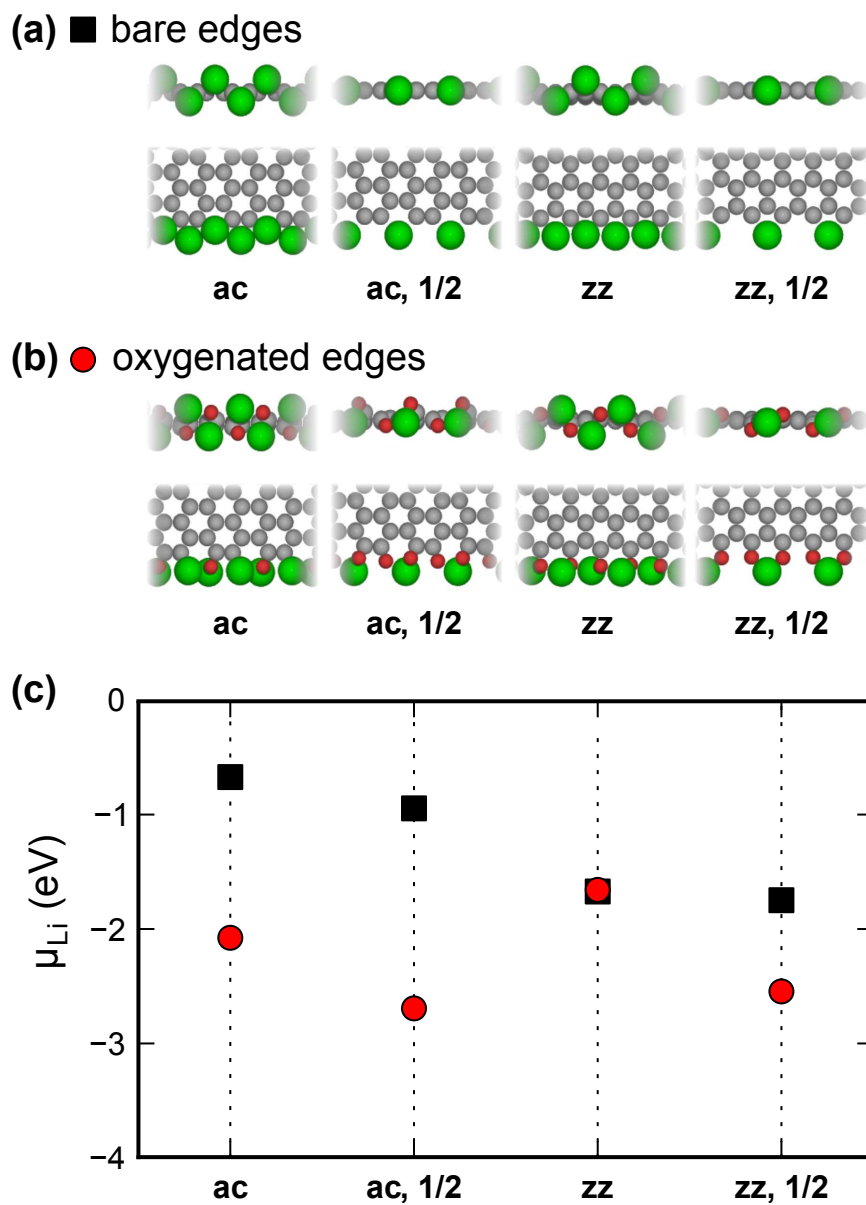


Figure 1: Ground-state configurations and Li^+ chemical potential μ_{Li} for Li^+ adsorbed bare graphene edges (squares) and carbonyl-terminated graphene edges (circles). Data is for zig-zag (zz) and armchair (ac) edges at full and half (1/2) coverage. Panel (a) shows the ground-state (minimum energy) configurations for bare edges, and (b) for carbonyl-terminated edges. Panel (c) shows the corresponding chemical potentials.

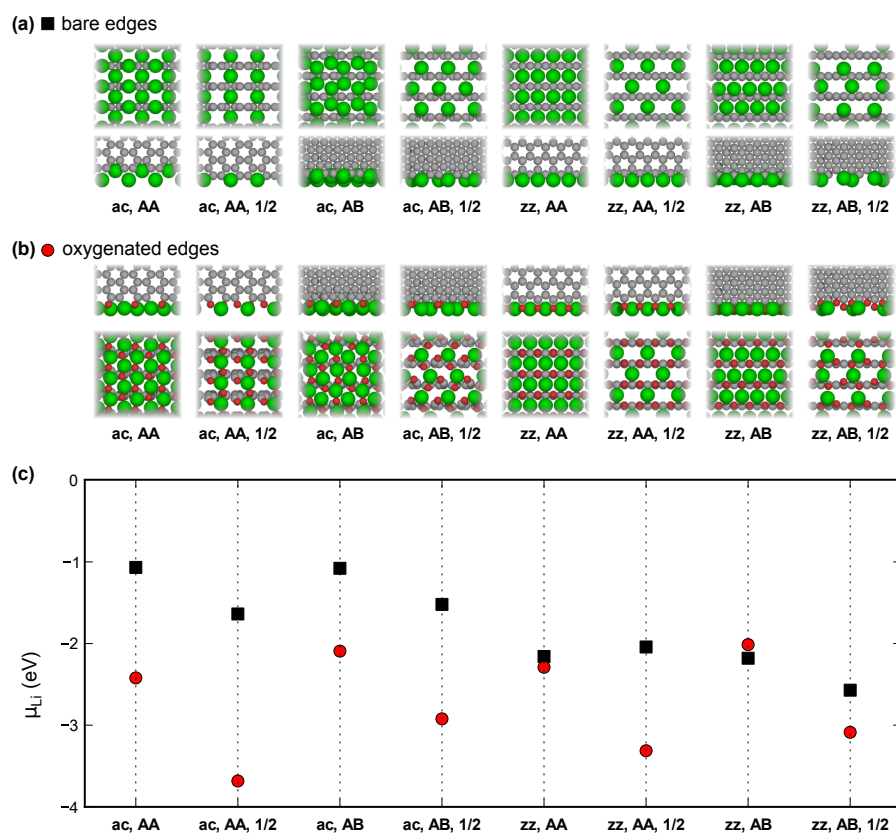


Figure 2: Ground-state configuration and Li^+ chemical potential μ_{Li} for lithium adsorbed on prismatic armchair (ac) and zig-zag (zz) surface of AA and AB stacked graphite. Shown are the results for bare (squares) and carbonyl-terminated surfaces (circles). Panel (a) shows the ground-state (minimum energy) configurations for bare edges, and (b) for carbonyl-terminated edges. Panel (c) shows the corresponding chemical potentials.

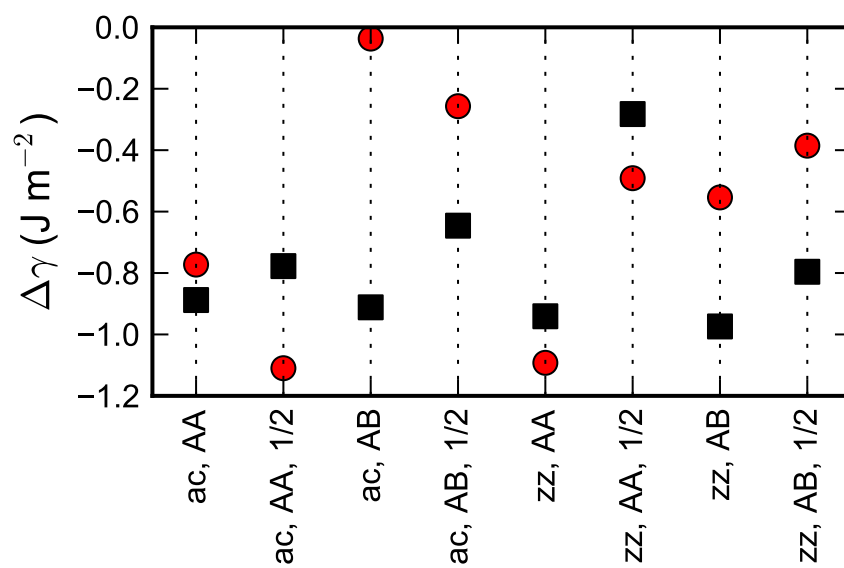


Figure 3: Gain in surface energy $\Delta\gamma$ upon lithium adsorption. Results are shown for prismatic bare (squares) and carbonyl terminated (circles) zig-zag (zz) and armchair (ac) surfaces.